CrossMark

Petrology and geochemistry of a boninite dyke from the western Bastar craton of central India

Biswajit Hazarika[1], D B Malpe[1] and Ashish Dongre[2],*

[1]*Department of Geology, RTM Nagpur University, Nagpur 440 001, India.*
[2]*Department of Geology, Savitribai Phule Pune University, Pune 411 007, India.*
Corresponding author. e-mail: andongrey@gmail.com

The Dongargarh Supergroup along with the basal Amgaon Gneissic Complex constitutes the northwestern part of the central Indian Bastar craton. In the present study, we report a new finding of a boninite dyke intruded in the Amgaon gneisses of this area. The dyke composed of mainly pyroxenes, amphiboles and subordinate amount of plagioclase. The higher contents of SiO_2 (51–54 wt.%), MgO (12–14 wt.%), Ni (375–473 ppm), Cr (1416–1580 ppm) and very low TiO_2 (0.2–0.4 wt.%) are consistent with the boninite nature of the dyke as well as the unevolved primary nature of the source magma. The extraordinarily high CaO content (15.97–17.7 wt.%) with higher CaO/Al_2O_3 (3.13–3.96) ratios classifies it as high-Ca boninite. The trace element ratios including Zr/Ti, Ti/V, Ti/Sc and Ti/Yb further show its geochemical similarity with the Archaean boninite. The dyke also shows negative high-field strength element (Nb, Ta and Ti) anomalies which are the characteristics of the boninite rocks reported elsewhere and along with the enriched light rare earth element pattern, it shows more affinity particularly with the northern Bastar boninite dyke. The mineralogical and geochemical similarities of the boninite dykes from the Bastar craton indicate a widespread boninitic event during the Palaeoproterozoic having a similar origin. These boninite dykes indicate the preservation of subduction-related signatures in the lithospheric mantle beneath the Bastar craton at the time of its evolution or may be during the convergence of the Bastar and Bundelkhand cratons.

Keywords. Boninite; petrology; subduction; Bastar craton; central India.

1. Introduction

Boninites are relatively rare, high MgO (>8 wt.%) and low TiO_2 (<0.5 wt.%) basaltic-to-andesitic rocks (Le Bas 2000). They are thought to form in the supra-subduction zone tectonic environment, derived from the shallow melting of a highly depleted hydrous mantle, fluxed with water from subducted slabs (e.g., Hickey and Frey 1982; Beccaluva and Serri 1988; Crawford *et al.* 1989; Stern and Bloomer 1992). However, they are also reported to form at the extended fore-arc with a scenario of propagation of back-arc spreading centres into the fore-arc regions (e.g., Manikyamba *et al.* 2005; Meffre *et al.* 2012), as well as the mantle plume interaction with the arc can also

be a possible scenario for the boninite formation (Falloon *et al.* 2007, 2008). The atypical geochemical characteristics of boninite point to its unusual genesis that includes high temperature (>1100°C) and involvement of subduction fluid in metasomatism of the shallow harzburgitic mantle, which was previously depleted by extensive extraction of tholeiitic melt (Crawford *et al.* 1989). The boninitic affinity of parental magmas for two of the world's largest platinum-group element deposits, the Bushveld igneous complex of South Africa and Stillwater complex of Montana, USA, manifest its economic importance (Crawford *et al.* 1989).

In the context of Indian subcontinent, boninites are reported from most of the cratons likewise the Singhbhum craton (Mir *et al.* 2015), Dharwar craton (Manikyamba *et al.* 2005; Ganguly *et al.* 2016) and Bastar craton (Srivastava 2006, 2008; Subba Rao *et al.* 2008a, b; Chalapathi Rao and Srivastava 2009). The Bastar craton contains the reports of the emplacement of boninitic rocks mostly in its southern and northern parts (Srivastava 2006; Subba Rao *et al.* 2008a, b), whereas a boninitic dyke is also reported from the Dongargarh Supergroup of rocks (Chalapathi Rao and Srivastava 2009). The aim of the present study is to report the occurrence of a boninite dyke for the first time from the western Bastar craton intruded in the Amgaon gneisses. The paper further discusses the geodynamic significance of this dyke based on the comprehensive petrological and geochemical studies.

2. Geological setting

The Archaean Bastar craton is one of the central Indian cratonic domains, which was separated from the Bundelkhand craton by the central Indian tectonic zone (CITZ) (Roy *et al.* 2000). The roughly rectangular-shaped Bastar craton, located south of the CITZ, is limited by NW–SE trending Mahanadi and Godavari rifts, ENE–WSW trending Narmada–Son rift and Eastern Ghats Mobile Belt. These rifts are considered to be formed during Precambrian (e.g., Naqvi and Rogers 1987; Srivastava *et al.* 2004). It lies in the ENE of the Dharwar craton, separated later by the Godavari rift. The overall tectonic trend of the craton is north–south, in contrast to ENE–WSW to east–west trend recorded in the Bundelkhand craton (Yedekar *et al.* 1990; Roy *et al.* 2000). The craton comprises granitoids and mafic

rocks, tonalite–trondhjemite gneisses, supracrustal rocks including greenstone belts and intrusive granitic plutons and unmetamorphosed Neoproterozoic sediments (Crookshank 1963; Ramakrishnan 1990; Chaudhuri *et al.* 2002; Srivastava *et al.* 2004; Ramakrishnan and Vaidyanadhan 2008). The craton has experienced different mafic magmatic events (volcanics and intrusives) during Precambrian that are reported from the different parts of the craton (Srivastava and Gautam 2009). Mafic volcanics are mostly represented by the basalts and basaltic andesites (Krishnamurthy *et al.* 1990; Neogi *et al.* 1996). However, the low-Ti and high-Ti volcanics and siliceous high magnesium basalts (SHMB) are also reported from the Palaeoproterozoic Dongargarh Supergroup (Asthana *et al.* 1996; Sensarma *et al.* 2002). Mafic intrusives of different ages and compositions are extensively reported from the southern, central and northern parts of the craton (e.g., Ramachandra *et al.* 1995; Srivastava and Singh 2004; Subba Rao *et al.* 2004, 2008a; Srivastava 2006; Mondal *et al.* 2007; French *et al.* 2008; Hussain *et al.* 2008; Srivastava and Gautam 2008, 2009, 2012; Ratre *et al.* 2010; Das *et al.* 2011; Srivastava *et al.* 2011; Gautam and Srivastava 2011; Sinha *et al.* 2011; Pisarevsky *et al.* 2013). The intrusives include sub-alkaline mafic dykes i.e., Bastar Dykes 1 (BD1 of ~2.7 Ga) and Bastar Dykes 2 (BD2 of 1.88–1.89 Ga), boninite–norite dykes (~2.1 Ga) from the southern part (French *et al.* 2008; Srivastava 2008; Srivastava *et al.* 2011), Bhanupratappur–Keshkal dykes from the central part (Ramachandra *et al.* 1995; Gautam and Srivastava 2011; Srivastava and Gautam 2012) and Dongargarh, Chhura, Lakhna (~1.44 Ga) and Bandimal (~1.42 Ga) dykes from the northern part of the craton (Ratre *et al.* 2010; Das *et al.* 2011; Sinha *et al.* 2011; Pisarevsky *et al.* 2013; Srivastava and Gautam 2015).

The boninite of the present study (21°28′40.3″N and 80°29′56″E) found as intrusive within the Amgaon gneisses of western Bastar craton (figure 1). This part of the craton mostly comprises the Amgaon Group and Dongargarh Supergroup of rocks. The Amgaon Group is composed of psammitic–psamopelitic metamorphite alternating with metabasic lavas. Granite gneisses along with TTG gneissic phase forms basement for the Dongargarh Supergroup (Sarkar *et al.* 1981; Rao 1981; Krishnamurthy *et al.* 1988; Sarkar 1994; Wanjari *et al.* 2005; Ramakrishnan and Vaidyanadhan 2008). The Neoarchean–Palaeoproterozoic Dongargarh Supergroup comprises older bimodal volcanics
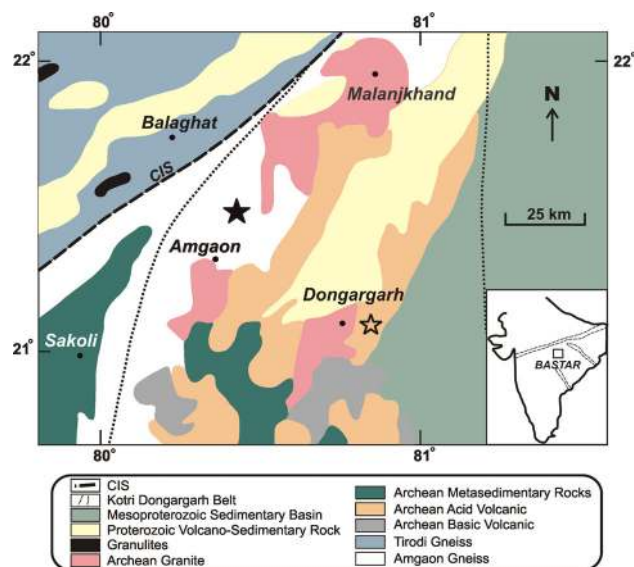
Figure 1. Geological map of the western Bastar craton, central India (after Asthana *et al.* 2017). Black asterisk represents the location of the present boninite dyke and the other one represents the location of Dongargarh boninite (Chalapathi Rao and Srivastava 2009).

of the Nandgaon Group and younger volcano-sedimentary sequence of the Khairagarh Group divided by an unconformity after the Dongargarh granitoid emplacement (Krishnamurthy *et al.* 1990).

3. Analytical technique

The mineral chemistry was determined using a Cameca SX 100 electron probe micro-analyser (EPMA) at the University of Johannesburg, South Africa. Quantitative mineral analyses were operated at 20 kV accelerating voltage, 20 nA beam current and $1\,\mu$m beam diameter with variable (12–40 s) counting time on the peak, based on the element. The standards used for the calibration of EPMA were natural jadeite (Na), olivine (Mg), almandine (Al), diopside (Si), orthoclase (K), wollastonite (Ca), rhodonite (Mn) and haematite (Fe), and synthetic pure oxides for TiO_2, Cr_2O_3 and NiO. Elements were measured on their $K\alpha$ lines. The 'X-PHI' method was used for the matrix correction (Merlet 1994). Backscattered electron (BSE) imaging was performed on the same instrument using the same conditions of acceleration voltage and beam current.

For the whole-rock chemical analyses, powdered rock samples were milled in HERZOG swing grinding mill (Model HSM-100) and were analysed using the fused disc and the borate fusion method. Major

element oxides for five samples were determined by inductively coupled plasma-emission spectrometry technique (SpectroCiros-CCD) at Acme Laboratories Canada and wavelength dispersive X-ray fluorescence spectrometry at Wadia Institute of Himalayan Geology, Dehradun. Trace elements (including rare earth elements (REEs)) were analysed by inductively coupled plasma-mass spectrometry (Perkin Elmer SCIEX, Model ELAN® 9000). Instruments were calibrated using the standard reference materials and internal standards, and accuracy was monitored using the certified reference materials using the fundamental parameters model. The analyses of the standard reference materials are given in table S1 (online supplementary material) to show the accuracy and precision of the present data.

4. Petrography

Petrographic studies reveal fine-to-medium-grained nature of the rock. Mineralogically, it mainly consists of pyroxenes with minor amounts of amphiboles and plagioclase (figure 2). Pyroxenes are represented by subhedral-to-anhedral grains of both clinopyroxenes (cpx) and orthopyroxenes (opx). Clinopyroxenes are dominant than orthopyroxenes. Patches of orthopyroxenes occurring as relict granulations in clinopyroxenes suggest their earlier formation. At some places, orthopyroxenes are replaced by amphiboles. Chloritisation effects are not predominant. Plagioclase grains occur as intercumulus by occupying the spaces between pyroxene grains. It shows albite twinning and some twin lamellae are deformed or disappeared, indicating the deformation of the grains (figure 2). Saussaritisation and sericitisation at the grain boundaries suggest an alteration.

5. Mineral chemistry

The mineral chemical compositions of clinopyroxenes and amphiboles are given in table 1.

5.1 *Clinopyroxene*

Clinopyroxene is a major mineral constituent of the dyke. It shows a narrow range of Mg number [Mg# = Mg/(Mg + Fe) atomic] between 0.76 and 0.78 and is mostly diopside in composition ($Wo_{48.5-50.1}-En_{38.2-39.2}-Fs_{11.5-12.3}$). These clinopyroxenes are more enriched in Ca compared
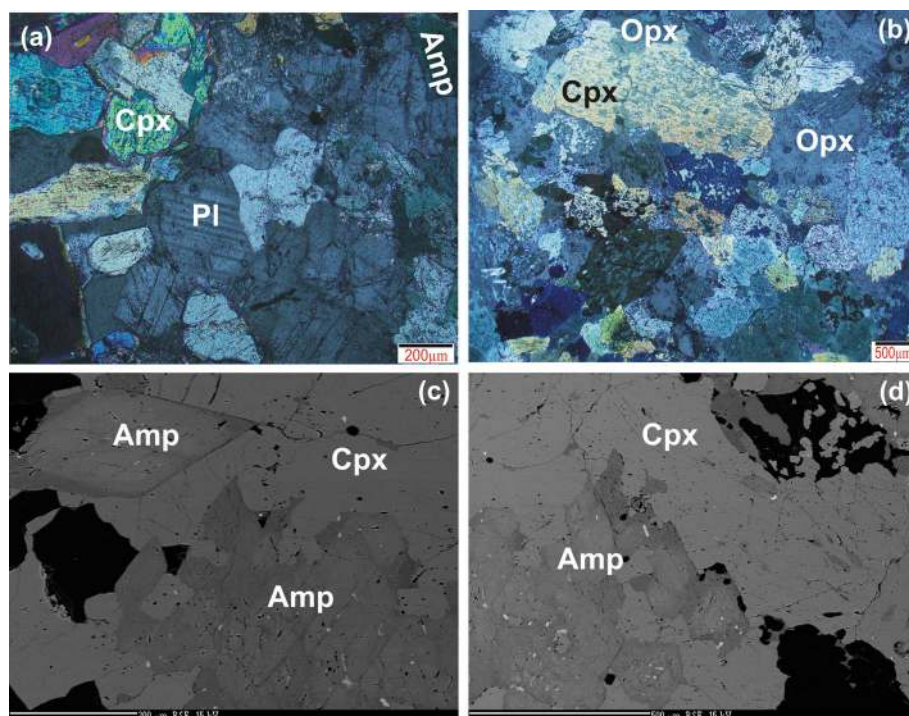
Figure 2. (**a**) Photomicrograph showing the presence of Cpx, Pl and Amp; (**b**) patches of Opx are visible in Cpx, at some places Opx breaks down to amphibole; (**c** and **d**) BSE images of present dykes showing Cpx and Amp grains. Abbreviations: Pl, plagioclase; Cpx, clinopyroxene; Amp, amphibole.

to the clinopyroxenes of the mafic Deccan basaltic rocks (Melluso and Sethna 2011) and are showing more similarity with the composition of the Dongargarh boninitic dyke (figure 3). The extremely low TiO_2 (0.02–0.09 wt.%) content of clinopyroxene is also similar to the boninitic dyke of the Dongargarh Supergroup (Chalapathi Rao and Srivastava 2009).

5.2 *Amphibole*

The amphiboles of the present study are mainly Ca-bearing and consist of high (>5 wt.%) and low alumina (<5 wt.%) variety. They are classified as actinolite and hornblende on the basis of Mg/(Mg+Fe) and Si (a.p.f.u.) contents (Leake *et al.* 1997) (figure 4). Chalapathi Rao and Srivastava (2009) reported the amphiboles of actinolite and hornblende composition from the boninitic dyke of Dongargarh Supergroup rocks, which are mostly showing similar composition with little enrichment in Mg content.

6. Bulk rock geochemistry

The major and trace element compositions of the studied dyke along with the average compositions of earlier reported boninite dykes from the Bastar craton of the central India (Srivastava 2006; Subba Rao *et al.* 2008a, b; Chalapathi Rao and Srivastava 2009), from Gadwal greenstone belt of south India (Manikyamba *et al.* 2005) and the Archaean boninites (Smithies *et al.* 2004) are given in table 2. The characteristic higher SiO_2 (>51.8−53.6 wt.%) and MgO (>12.2−14.3 wt.%) contents and higher Mg number (Mg# = Mg + Fe/Mg) of 73–76 shown by the present dykes are similar to the earlier reported worldwide boninitic rocks. The high Mg-rock classification schemes recommended by IUGS (Le Bas 2000), based on the total alkali *vs.* SiO_2 content, classify the present samples as boninites and are showing very similar composition to the earlier reported Bastar boninites (Srivastava 2006; Subba Rao *et al.* 2008a, b; Chalapathi Rao and Srivastava 2009) (figure 5). The dyke shows extremely elevated CaO content (15.9–17.7 wt.%) as compared to the earlier reported boninites from the Bastar craton. The SiO_2, Al_2O_3 and Na_2O contents show a negative correlation with MgO, while the TiO_2 increases with the increasing MgO (figure 6a–d), which is consistent with the fractionation trends in the mafic magma and with the other boninites. The normal trends of major oxides with MgO also suggest their immobility during alteration or metamorphic processes.

Table 1. *Chemical compositions (EPMA results), and calculated mineral formulae of the amphibole and clinopyroxene in the boninite dyke of the present study.*

Mineral					Amphibole						
Analysis no.	AMG-11/3	AMG-11/5	AMG-11/8	AMG-11/10	AMG-11/1	AMG-11/2	AMG-11/4	AMG-11/6	AMG-11/7	AMG-11/9	AMG-11/11
Major oxides (wt.%)											
SiO_2	51.84	53.65	54.83	52.56	50.11	50.23	50.89	49.73	47.98	49.81	49.94
TiO_2	0.33	0.1	0.06	0.12	0.61	0.43	0.29	0.36	0.77	0.56	0.42
Al_2O_3	4.13	3.01	2.21	3.53	5.38	5.4	4.96	6.11	7.5	5.62	5.53
FeO	11.79	10.93	10.21	11.26	12.54	12.48	12.03	12.78	13.92	12.52	12.65
MnO	0.18	0.16	0.16	0.18	0.19	0.15	0.15	0.19	0.19	0.16	0.17
MgO	15.33	16.36	17.25	16.06	14.43	14.4	14.79	14.07	13.13	14.5	14.69
CaO	12.82	12.73	13.1	12.9	12.67	12.79	12.78	12.65	12.82	12.6	12.79
Na_2O	0.64	0.43	0.26	0.48	0.86	0.79	0.71	0.9	1.11	0.82	0.78
K_2O	0.32	0.18	0.12	0.22	0.41	0.45	0.35	0.44	0.56	0.4	0.42
F	0.13	0.08	0.09	0.09	0.1	0.11	0.11	0.12	0.1	0.1	0.1
Cl	0.02	0.01	0	0.02	0.07	0.04	0.02	0.07	0.07	0.04	0.05
Total	97.53	97.64	98.29	97.42	97.37	97.27	97.08	97.42	98.15	97.13	97.54
Calculated mineral formulae (a.p.f.u.)*											
Coef.	8.70	8.60	8.51	8.66	8.77	8.78	8.76	8.78	8.81	8.79	8.77
Si	7.50	7.68	7.76	7.58	7.32	7.34	7.42	7.27	7.03	7.29	7.29
Ti	0.04	0.01	0.01	0.01	0.07	0.05	0.03	0.04	0.08	0.06	0.05
Al	0.70	0.51	0.37	0.60	0.93	0.93	0.85	1.05	1.30	0.97	0.95
Fe^{2+}	1.43	1.31	1.21	1.36	1.53	1.52	1.47	1.56	1.71	1.53	1.54
Mn	0.02	0.02	0.02	0.02	0.02	0.02	0.02	0.02	0.02	0.02	0.02
Mg	3.31	3.49	3.64	3.45	3.14	3.14	3.21	3.07	2.87	3.16	3.20
Ca	1.99	1.95	1.99	1.99	1.98	2.00	2.00	1.98	2.01	1.98	2.00
Na	0.18	0.12	0.07	0.13	0.24	0.22	0.20	0.26	0.32	0.23	0.22
K	0.06	0.03	0.02	0.04	0.08	0.08	0.07	0.08	0.10	0.07	0.08
F	0.06	0.04	0.04	0.04	0.05	0.05	0.05	0.06	0.05	0.05	0.05
Cl	0.00	0.00	0.00	0.00	0.02	0.01	0.00	0.02	0.02	0.01	0.01
Total	15.29	15.17	15.13	15.24	15.37	15.36	15.31	15.41	15.51	15.37	15.40
XMg	0.70	0.73	0.75	0.72	0.67	0.67	0.69	0.66	0.63	0.67	0.67

Table 1. *(Continued.)*

Mineral	Clinopyroxene										
Analysis No.	AMG-11/1	AMG-11/2	AMG-11/3	AMG-11/4	AMG-11/5	AMG-11/6	AMG-11/7	AMG-11/8	AMG-11/9	AMG-11/10	AMG-11/11
Major oxides (wt.%)											
SiO_2	53.78	53.61	53.82	53.6	53.8	53.75	53.65	53.48	53.25	53.5	53.97
TiO_2	0.06	0.03	0.02	0.09	0.02	0.07	0.06	n.a.	0.04	0.04	0.03
Al_2O_3	0.53	0.55	0.26	0.53	0.45	0.58	0.5	0.36	0.47	0.61	0.48
FeO	7.47	7.17	7.17	7.62	7.32	7.26	7.27	7.19	7.35	7.63	7.35
MnO	0.23	0.22	0.25	0.2	0.2	0.23	0.2	0.22	0.24	0.21	0.2
MgO	13.68	13.69	13.96	13.91	13.67	13.77	13.89	13.82	13.78	13.78	13.72
CaO	24.47	24.39	25.03	23.97	24.85	24.42	24.56	25.12	24.6	24.34	24.68
Na_2O	0.35	0.35	0.22	0.43	0.28	0.33	0.31	0.28	0.33	0.33	0.32
K_2O	n.a.	0.01	0.01	0.01	n.a.	n.a.	0.01	0.01	n.a.	0.01	n.a.
F	0.06	0.05	0.02	0.02	0.03	0.03	0.04	n.a.	0.05	0.01	0.02
Cl	0.01	0.01	0.01	n.a.	n.a.	n.a.	n.a.	n.a.	n.a.	0.01	n.a.
Total	100.64	100.08	100.77	100.38	100.62	100.44	100.49	100.48	100.11	100.47	100.77
Calculated mineral formulae (a.p.f.u.)[*]											
Coeff.	2.23	2.23	2.22	2.23	2.23	2.23	2.23	2.23	2.24	2.23	2.22
Si	1.99	1.99	1.99	1.99	1.99	1.99	1.99	1.99	1.98	1.99	1.99
Ti	n.a.	n.a.	n.a.	n.a.	n.a.	n.a.	n.a.	n.a.	n.a.	n.a.	n.a.
Al	0.02	0.02	0.01	0.02	0.02	0.03	0.02	0.02	0.02	0.03	0.02
Fe^{2+}	0.23	0.22	0.22	0.24	0.23	0.22	0.23	0.22	0.23	0.24	0.23
Mn	0.01	0.01	0.01	0.01	0.01	0.01	0.01	0.01	0.01	0.01	0.01
Mg	0.76	0.76	0.77	0.77	0.75	0.76	0.77	0.77	0.77	0.76	0.76
Ca	0.97	0.97	0.99	0.95	0.99	0.97	0.98	1.00	0.98	0.97	0.98
Na	0.03	0.03	0.02	0.03	0.02	0.02	0.02	0.02	0.02	0.02	0.02
F	0.01	0.01	n.a.	n.a.	n.a.	n.a.	n.a.	n.a.	n.a.	n.a.	n.a.
Cl	n.a.	n.a.	n.a.	n.a.	n.a.	n.a.	n.a.	n.a.	n.a.	n.a.	n.a.
Total	4.01	4.01	4.01	4.01	4.01	4.01	4.01	4.02	4.02	4.01	4.01
XMg	0.77	0.77	0.78	0.76	0.77	0.77	0.77	0.77	0.77	0.76	0.77
Calculated mineral fractions (mol%)[†]											
Wo	49.43	49.57	49.83	48.51	49.97	49.41	49.41	50.13	49.52	49.05	49.70
En	38.45	38.72	38.67	39.17	38.25	38.77	38.89	38.38	38.60	38.65	38.45
Fs	12.12	11.71	11.50	12.32	11.79	11.82	11.71	11.50	11.88	12.30	11.85

n.a.: not analysed or means below the EPMA detection limit; XMg = Mg/(Mg + Fe) atomic.
[*]Calculated on the basis of 23 (amphiboles) and 6 (clinopyroxenes) oxygen ions per formula unit, respectively.
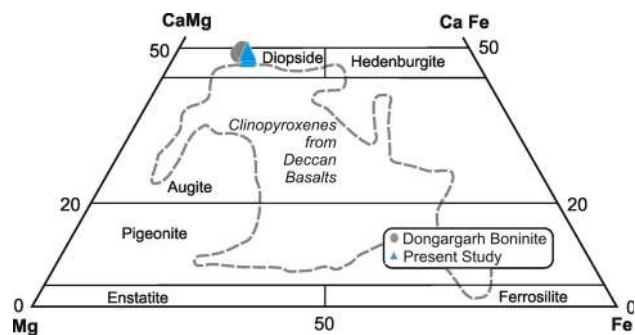[†]Abbreviations used for normative minerals. Wo: wollastonite; En: enstatite; Fs: ferrosilite.

Figure 3. Composition of pyroxenes in Ca–Mg–Fe diagram. Deccan basalts pyroxenes field is taken from Melluso and Sethna (2011) and data for Dongargarh boninites from Chalapathi Rao and Srivastava (2009).
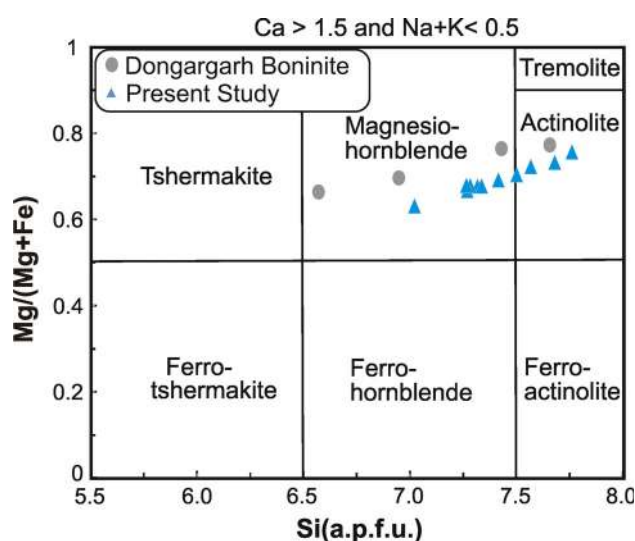

Figure 4. Compositional variation and classification of amphiboles (after Leake *et al.* 1997). Data for Dongargarh boninites from Chalapathi Rao and Srivastava (2009).

The present dyke shows high amounts of compatible trace elements such as Sc (49–50 ppm), V (228–230 ppm), Cr (1416–1580 ppm) and Ni (375–473 ppm). Nickel shows a positive correlation with MgO (figure 7a) like other boninite rocks and is consistent with the fractionation of the mafic magma. The Zr, Ti, Nb and V concentrations (figure 7b–d) are much more similar to the other reported boninites from Bastar and Dharwar cratons and particularly to the Archaean boninites (Smithies 2002). Nb concentration is between 2.2 and 2.7 ppm. The very low Nb values are reported from the Dongargarh boninites (0.18–0.23 ppm) (Chalapathi Rao and Srivastava 2009), whereas higher values (5–6 ppm) are known from the Bastar (Srivastava 2006; Subba Rao *et al.* 2008a, b) and Gadwal boninites (Manikyamba *et al.* 2005). Primitive mantle normalised multi-element diagrams

(normalising values after Sun and McDonough 1989) show enrichment of large ion lithophile elements (LILEs) as compared to high-field strength elements (HFSEs) with prominent negative anomalies at Nb, Ta, Zr, Hf and Ti (figure 8b). Chondrite normalised REE patterns (Sun and McDonough 1989) (figure 8a) show an enriched trend of light REEs (LREE) and a relatively depleted trend of heavy REEs (HREE) with distinct negative Eu anomaly indicating plagioclase fractionation during the evolution of the melt.

7. Discussion

The studied dyke shows higher MgO content (i.e., >12 wt.%) and compatible trace elements (Sc, V, Cr and Ni) which indicates the primary nature of its source magma. The higher amount of MgO and lower Al_2O_3, K_2O, Na_2O, Rb and Sr demonstrate that the dyke is not affected by the significant crustal contamination. The intrusion of dyke in the gneisses would have been elevated these element concentrations on the event of crustal contamination. The Al and Ti contents of boninites along with the trace elements such as Th, Nb, Ta, Zr, Hf, Y, Sc and V are considered to be least susceptible to alteration and conventionally used to differentiate various high-Mg mafic rocks such as boninite, high-Mg norite, SHMB and komatiite (Poidevin 1994; Piercey *et al.* 2001; Polat *et al.* 2002; Smithies 2002; Srivastava 2006; Chalapathi Rao and Srivastava 2009). The very low values of Nb/La (0.15–0.22), Nb/Ce (0.07–0.08) Rb/Sr (0.01–0.05) and Rb/Ba (0.04–0.07) showed by the present dyke also rule out the effects of post-magmatic deuteric alteration processes as well as crustal contamination (Lafleche *et al.* 1992; Mir *et al.* 2011). The negative Nb, Ta and Ti anomalies on multi-element diagram are common features in the Archaean as well as Phanerozoic boninites (Smithies *et al.* 2004) and also characteristic of the magmatism related to subduction (Wilson 1989; Condie 1997). The relative depletion in the HFSEs (Nb, Ta and Ti) may have been affected by crustal contamination; however, these anomalies are consistent in the global boninitic rocks and it looks like much of these and the overall trace element signatures may have been largely inherited from the enriched sources (Cameron *et al.* 1983; Hall and Hughes 1990; Nielsen *et al.* 2002; Smithies 2002; Srivastava 2006).

Table 2. *Bulk rock chemical compositions of the dyke under study and compilation of earlier reported boninite compositions.*

Sample no.	1 AMG-10	2 AMG-11	3 DMK 2541	4 DMK 2543	5 DMK 2544	6 DB (n = 2)	7 NBB (n = 6)	8 SBB (High-Ca; n = 3)	9 SBB (Low-Ca; n = 24)	10 GB (n = 22)	11 AB (n = 15)
Major oxides (wt.%)											
SiO_2	53.57	52.32	52.11	51.84	53.62	51.79	56.03	53.41	53.57	48.73	51.25
TiO_2	0.31	0.37	0.35	0.24	0.19	0.04	0.33	0.32	0.46	0.28	0.34
Al_2O_3	5.27	4.47	5.14	4.27	4.51	6.14	9.38	12.80	10.92	10.33	16.36
Fe_2O_3	7.89	9.04	8.07	9.32	7.81	8.41	9.62	9.17	10.81	11.64	10.19
MnO	0.14	0.17	0.13	0.19	0.22	0.14	0.17	0.15	0.17	0.15	0.18
MgO	12.20	12.90	13.53	14.34	13.17	18.56	11.75	10.02	13.03	18.74	7.81
CaO	16.51	17.70	16.85	15.97	16.34	12.17	8.56	12.29	6.50	9.32	9.96
Na_2O	1.62	1.05	1.27	1.14	1.57	0.51	2.17	1.24	1.23	0.64	1.70
K_2O	0.41	0.20	0.31	0.45	0.27	0.30	0.84	0.12	0.93	0.42	0.43
P_2O_5	0.03	0.04	0.06	0.04	0.07	0.05	0.09	0.05	0.07	0.03	0.04
LOI	1.50	1.20	1.65	1.35	1.43	1.63	–	0.63	2.21	4.11	3.51
Total	99.45	99.46	99.47	99.15	99.20	99.73	99.04	99.56	97.70	104.09	101.74
CaO/Al_2O_3	3.13	3.96	3.28	3.33	3.62	1.99	0.93	1.02	0.59	0.90	0.49
Mg#	76.43	74.96	74.93	73.28	75.04	81.45	68.25	71.37	70.71	77.45	64.53
Trace elements (ppm)											
Sc	49	50	–	–	–	56.66	41.50	36.67	30.46	42.91	44.08
V	228	230	–	–	–	218.50	194.00	168.33	173.38	94.05	167.38
Cr	1580.50	1416.29	–	–	–	2677.50	1181.17	1169.50	1229.93	2008.41	595.54
Co	45.2	50.3	–	–	–	70.94	68.50	–	–	76.59	70.43
Ni	375	473	–	–	–	362.00	157.17	274.50	303.87	838.73	248.77
Ga	10.2	8.7	–	–	–	11.78	21.83	6.50	6.25	–	–
Rb	7.6	1.5	–	–	–	7.35	56.67	3.00	47.33	58.73	20.92
Sr	154.2	131.2	–	–	–	203.00	241.67	100.33	78.54	33.82	100.31
Y	8.4	12.7	–	–	–	10.93	17.17	9.33	12.71	13.41	11.07
Zr	49.8	46	–	–	–	26.16	58.00	40.67	63.25	16.64	29.07
Nb	2.2	2.7	–	–	–	0.21	3.00	1.00	3.63	0.79	1.14
Cs	0.08	0.07	–	–	–	0.10	1.67	–	–	7.06	–
Ba	115	37	–	–	–	158.50	267.00	66.33	180.21	39.27	82.42
Hf	1.4	1.4	–	–	–	0.69	1.23	0.90	1.88	0.45	–
Ta	0.2	0.1	–	–	–	0.05	0.69	0.14	0.59	0.06	–
Th	2.3	2.4	–	–	–	0.66	3.50	1.45	5.20	0.27	0.45
U	0.5	0.5	–	–	–	0.23	1.50	–	–	0.14	0.17
Ti	1858.45	2218.15	–	–	–	239.00	1988.24	1938.38	2727.73	1651.35	2022.31
REE (ppm)											
La	14.8	12.5	–	–	–	5.33	14.90	5.95	10.73	2.00	2.87

	1	2	3	4	5	6	7	8	9	10	11
Ce	6.44	4.11	22.13	10.50	27.99	12.13	—	—	—	31.6	33
Pr	0.83	0.56	2.32	1.07	2.84	1.96	—	—	—	3.93	4.47
Nd	3.48	2.44	9.06	4.45	13.21	9.24	—	—	—	16.1	19.6
Sm	0.91	0.69	1.97	1.05	2.73	2.22	—	—	—	3.59	4.29
Eu	0.31	0.29	0.53	0.35	0.85	0.73	—	—	—	0.83	0.96
Gd	1.13	1.09	2.08	1.25	2.84	2.49	—	—	—	3.08	3.68
Tb	0.22	0.26	0.38	0.25	0.42	0.38	—	—	—	0.4	0.53
Dy	1.59	1.87	2.17	1.50	2.57	1.85	—	—	—	1.94	2.77
Ho	0.39	0.49	0.45	0.35	0.54	0.42	—	—	—	0.31	0.48
Er	1.26	1.44	1.36	1.00	1.61	1.19	—	—	—	0.88	1.39
Tm	0.25	0.48	0.23	0.16	0.22	0.18	—	—	—	0.12	0.18
Yb	1.45	1.49	1.37	0.95	1.33	1.02	—	—	—	0.74	1.1
Lu	0.23	0.24	0.22	0.15	0.26	0.16	—	—	—	0.1	0.15
Total REE	21.24	17.44	48.05	28.98	72.31	39.26	—	—	—	78.42	85.1
Ti/V	11.97	19.25	15.74	11.51	10.37	1.10	—	—	—	8.15	9.64
Ti/Sc	44.61	47.63	89.68	54.63	48.94	4.23	—	—	—	37.93	44.36
Ti/Yb	1552.68	1126.19	1957.93	1846.19	1516.81	236.76	—	—	—	2511.42	2016.50

1–5: Present study; 6: Dongargarh boninite (DB) (Chalapathi Rao and Srivastava 2009); 7: northern Bastar boninite (NBB) (Subba Rao et al. 2008a, b); 8–9: southern Bastar boninite (SBB) (Srivastava 2006); 10: Gadwal boninite (GB) (Manikyamba et al. 2005); 11: Archaean boninite (AB) (Smithies et al. 2004).

–: not analysed; Mg# = atomic $Mg/(Mg + Fe^{2+}) \times 100$. LOI: loss on ignition.

Global boninites have a marked U-shape (depleted middle REE (MREE) than the LREE and HREE) multi-element pattern (Bedard 1999; Polat *et al.* 2002; Manikyamba *et al.* 2005). Such a depleted MREE pattern is not observed in the present dyke and remains absent in the Bastar craton boninites. Whereas the depleted HREEs compared to LREE and MREE patterns are observed to be a characteristic feature of all the Bastar boninites (Subba Rao *et al.* 2008a; Chalapathi Rao and Srivastava 2009).

The CaO content of the present dyke is very high that it ranges from 15.9 to 17.7 wt.%, which is higher compared to the Proterozoic boninites of the Bastar craton and Gadwal greenstone belt. The Al_2O_3 content of the dyke is very low; however, the lower Al_2O_3 and higher CaO are the characteristics of the nearby Dongargarh boninite from the same Bastar craton and considered here to be distinct features of these dykes. Very low CaO values (i.e., 0.10–0.12 wt.%) are characteristics of the Archaean boninites (Smithies 2002). Based on the lower amounts of Al_2O_3 and higher CaO/Al_2O_3 ratios, the present dyke is classified, more precisely, as a high-Ca boninite variety (figure 9). The phanerozoic boninites generally show a very high Al_2O_3/TiO_2 ratio and in Archaean boninites such ratio varies from 26 to 88. The value of Al_2O_3/TiO_2 in the present dyke varies
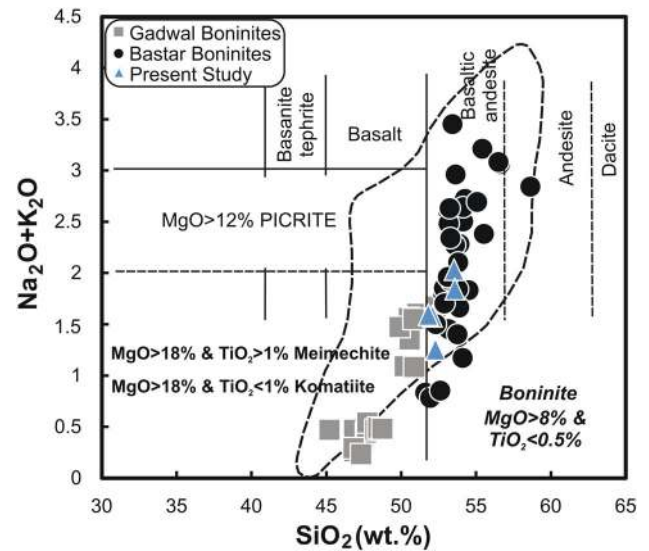

Figure 5. Total alkali silica (TAS) classification diagram (after Le Bas 2000) for high-Mg mafic dykes and compositional variation of present dyke is compared with the Archaean boninite field (Smithies *et al.* 2004), Bastar boninites (Srivastava 2006; Subba Rao *et al.* 2008a, b; Chalapathi Rao and Srivastava 2009) and Gadwal boninites (Manikyamba *et al.* 2005).

from 12 to 24. The lower Al_2O_3/TiO_2 values can be attributed to the lower content of Al_2O_3 in the present dyke, which is also a feature of Dongargarh boninite as mentioned earlier. On the other hand, TiO_2 contents of the dyke are very low (0.19–0.37 wt.%) and following the boninite classification where TiO_2 is mostly <0.5 wt.%. The bivariate plots, using Zr/Ti, Ti/V, Ti/Sc and Ti/Yb ratios (figure 10a–d) discriminating between Archaean boninites with contaminated komatiites and SHMB, show a distinct affinity of the studied samples towards the Archaean boninites.

Smithies *et al.* (2004) recognised two groups of Archaean high-Mg mafic rocks having strong refractory mantle source, e.g., Whundo type and Whitney type. Whundo type (known in age from 3.12 and 2.8 Ga) rocks are considered to be true Archaean analogues of modern boninites, having similarities in the composition and also their association with tholeiitic to calc-alkaline mafic to intermediate magmatism. They are similar to modern boninites in terms of their derivation from the metasomatised refractory mantle. On the other hand, Whitney type (of 3.8 Ga) rocks are closely associated with ultramafic komatiites and are considered to be derived by plume magmatism. Pearce *et al.* (1992) suggested the genesis of boninites by melting of depleted residual metasomatic MORB

mantle where metasomatism is due to fluids and melts are derived from the dehydrated subducted slab. Earlier studies (e.g., Arndt *et al.* 1987; Sun *et al.* 1989) reported the role of assimilation-fractional crystallisation (AFC) of komatiites for the formation of boninites. The present dyke represents a Whundo type of magmatism and is not consistent with a komatiite AFC model in its genesis because of no record of komatiite in the vicinity.

The formation of boninites by higher degrees of partial melting of a refractory mantle source related to the subduction is now well established (Tatsumi and Eggins 1995; Turner *et al.* 1997; Green and Falloon 1998; Falloon and Danyushevsky 2000; Kushiro 2007). Very low contents of titanium are considered to be due to residual Ti-bearing phase after melting (Green and Pearson 1986) in the refractory mantle source formed by the tholeiitic melt extraction (Sun and Nesbitt 1978). Subsequent enrichment of refractory mantle source regions and higher concentrations of LILEs, Th and La compared to HFSEs are considered to be the result of interaction with subduction-derived fluid prior to the second-stage melting (Sun and Nesbitt 1978; Hickey and Frey 1982; Crawford *et al.* 1989; Falloon and Danyushevsky 2000; Polat *et al.* 2002; Smithies *et al.* 2004).
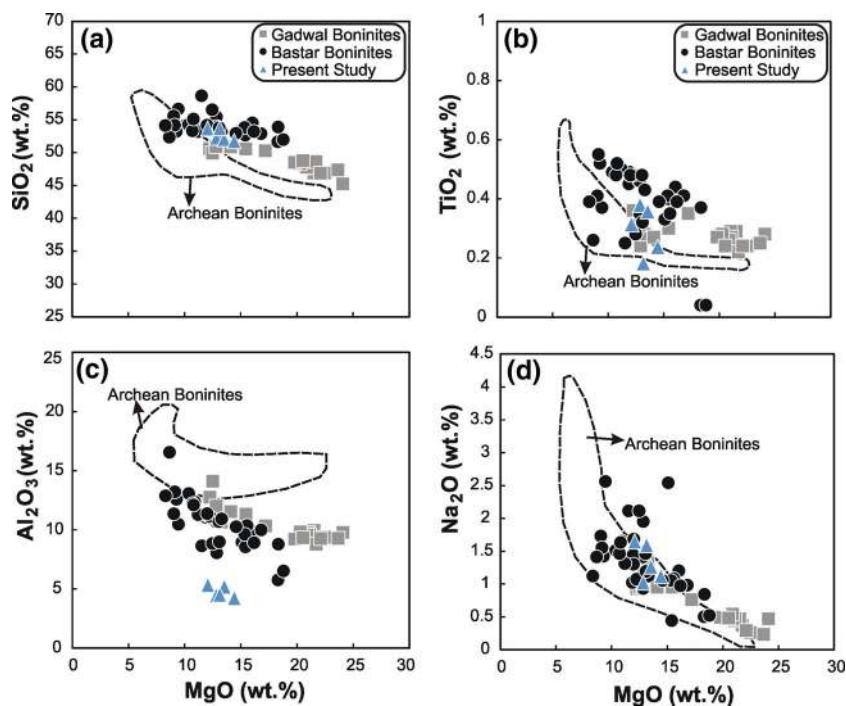

Figure 6. (**a–d**) Variations of major oxides (SiO_2, TiO_2, Al_2O_3 and Na_2O) with MgO (wt.%) and are compared with earlier reported Archaean boninites (Smithies *et al.* 2004), Bastar boninites (Srivastava 2006; Subba Rao *et al.* 2008a, b; Chalapathi Rao and Srivastava 2009) and Gadwal boninites (Manikyamba *et al.* 2005).
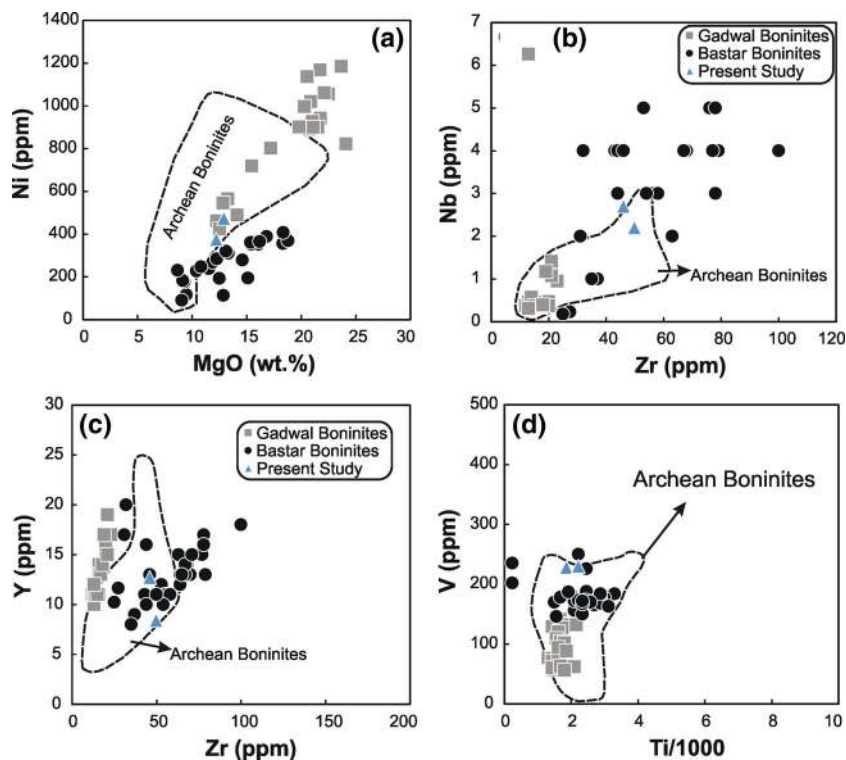
Figure 7. (**a**) MgO (wt.%) *vs.* Ni (ppm); (**b**) Zr (ppm) *vs.* Nb (ppm); (**c**) Zr (ppm) *vs.* Y (ppm); and (**d**) Ti/1000 *vs.* V (ppm) variation diagrams for the present boninite dyke and their comparison with earlier reported Archaean boninites (Smithies *et al.* 2004), Bastar boninites (Srivastava 2006; Subba Rao *et al.* 2008a, b; Chalapathi Rao and Srivastava 2009) and Gadwal boninites (Manikyamba *et al.* 2005).

The formation of boninitic dykes from a refractory mantle source and subduction-induced metasomatism have been known from the Bastar craton (Srivastava 2008; Chalapathi Rao and Srivastava 2009) and the neighbouring Singhbhum craton (Mir *et al.* 2015). It was suggested that the extensive extraction of tholeiitic melt during Archaean to Palaeoproterozoic (Srivastava and Gautam 2009) may have resulted in the formation of refractory mantle sources beneath the Bastar craton and the subduction-related tectonic settings (Yedekar *et al.* 1990; Asthana *et al.* 2016) could be the reason for geochemical characteristics typical of boninite shown by these rocks.

The samples under the study show very low TiO_2 contents (i.e., <0.40 wt.%) with correspondingly higher CaO/TiO_2 ratios (47.84–86.00) indicate their highly refractory mantle source which had experienced earlier the tholeiitic melt extraction event. The enriched Ce/Ta ratios (158–330) along with negative HFSE anomalies reflect the contribution of subduction-related component in the melt (Smellie *et al.* 1995) and thus support the role of subduction in influencing the geochemical

characters of the present boninite dyke in the western part of the Bastar craton.

7.1 *Geodynamics involved*

Boninite dyke emplaced in the Archaean basement was reported from the margin of the Chhattisgarh basin in the northern Bastar craton (Subba Rao *et al.* 2008a, b). This dyke inferred to form in intra-cratonic settings, similar to other Archaean boninite rocks reported from other parts of the world (e.g., Smithies 2002). Boninite dyke reported from the Neoarchean–Palaeoproterozoic Dongargarh Supergroup is intrusive into the Bijli rhyolites in northwestern Bastar craton (Chalapathi Rao and Srivastava 2009) and is considered to represent a fossil subduction zone where a lithospheric mantle in this domain appears to have retained memories of ancient subduction. Palaeoproterozoic boninites are reported from the southern Bastar craton which are intrusives into basement gneisses (Srivastava and Singh 2003; Srivastava *et al.* 2004, 2011) and also from the areas of Bastanar, Dantewada and Katekalyan of southern Bastar craton
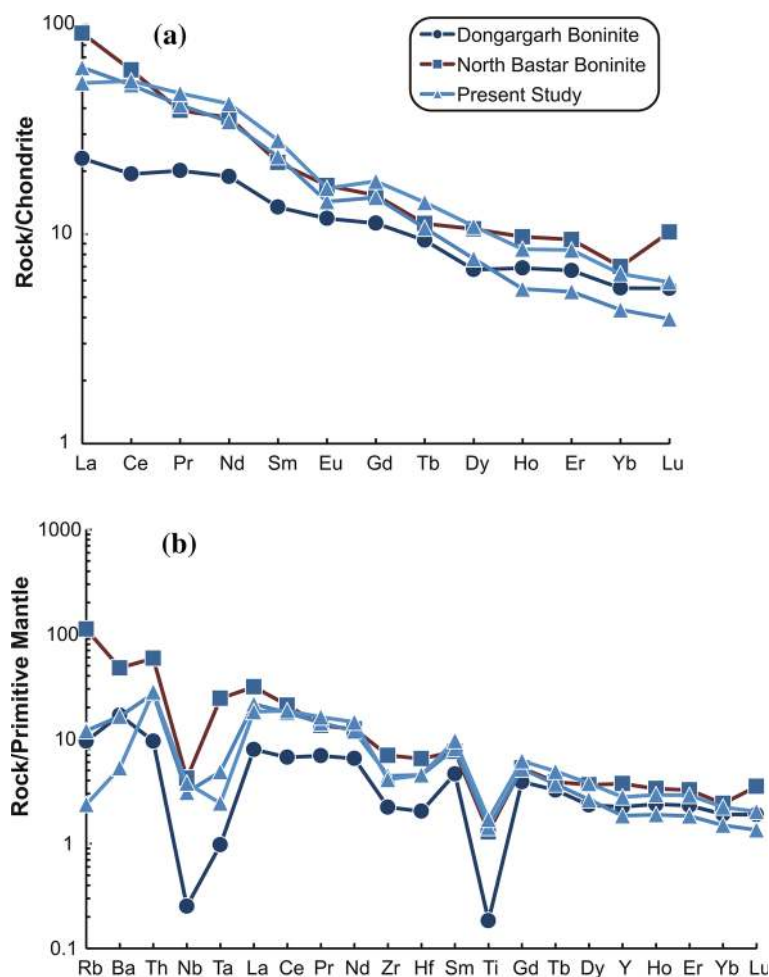
Figure 8. (**a**) Chondrite-normalised (after Sun and McDonough 1989) and (**b**) primitive-mantle normalised (after Sun and McDonough 1989) patterns for the present study dyke and boninite dykes from the north Bastar craton (Subba Rao *et al.* 2008a, b) and Dongargarh boninite dyke (Chalapathi Rao and Srivastava 2009).

(Srivastava 2006) where they are very well exposed. These dykes are also reported to form in an intra-cratonic setting. This clearly indicates the presence of widespread intra-cratonic boninite magmatism in the whole Bastar craton during Neoarchean to Palaeoproterozoic.

A number of geodynamic models have been proposed for the evolution of central Indian Neoar-chean–Palaeoproterozoic Dongargarh Supergroup rocks (e.g., Yedekar *et al.* 1990; Raza *et al.* 1993; Neogi *et al.* 1996; Asthana *et al.* 1996, 1997, 2016, 2017; Manikyamba *et al.* 2016). Yedekar *et al.* (1990) envisaged the Dongargarh volcanic rocks as remnant island arc lavas and proposed a southward subduction model of the Bundelkhand proto-continent under the Deccan proto-continent during the Proterozoic. Raza *et al.* (1993) also supported the subduction-related origin of the Dongargarh volcanics that exist along a Palaeopro-terozoic ocean closure in central India and mark the

suture of two proto-continental masses. Asthana *et al.* (1996, 1997) suggested an arc-related set-ting for Khairagarh volcanics of the Dongargarh Supergroup, which are inter-layered with terrige-nous sediments formed in back-arc basin. In recent works, Asthana *et al.* (2016, 2017) proposed a ridge subduction model followed by slab window along Palaeoproterozoic central Indian suture to account for the distribution of fore arc–arc–back arc asso-ciation of the Bastar craton. Geochemical studies on gneisses and granitoids also provide significant evidence for the multiphase subduction-related events and for crustal growth during Protero-zoic and Archaean in the Bastar craton (Hussain *et al.* 2004; Mondal *et al.* 2006). Therefore, the convergence-related evolution of the Bastar cra-ton and especially the Dongargarh Supergroup is clearly established from the previous studies.

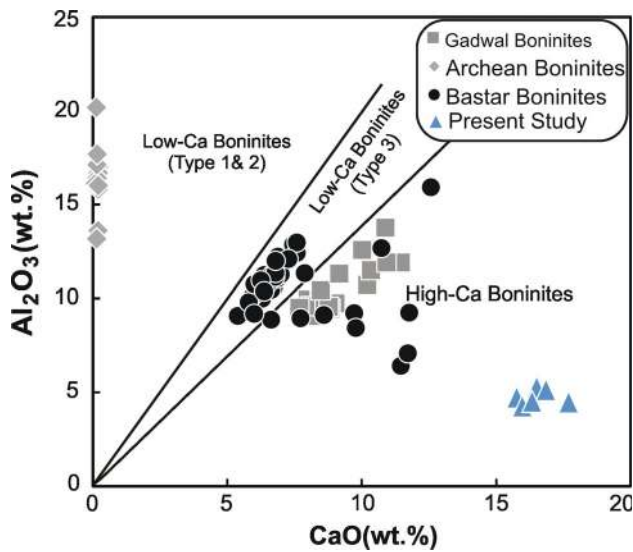The present boninite dyke is intrusive into the Amgaon gneisses and not in the Dongargarh

Figure 9. CaO/Al_2O_3 classification for boninites (Crawford *et al.* 1989). Boninite compositions from earlier reports such as Archaean boninite field (Smithies *et al.* 2004), Bastar boninites (Srivastava 2006; Subba Rao *et al.* 2008a, b; Chalapathi Rao and Srivastava 2009) and Gadwal boninites (Manikyamba *et al.* 2005) are also given for comparison.

Supergroup rocks unlike the Dongargarh boninite reported by Chalapathi Rao and Srivastava (2009). The Amgaon gneisses of the western Bastar craton shows widespread ages of 2.5–2.6 Ga (Ramakrishnan and Vaidyanadhan 2008) and forms the basement for the Dongargarh Supergroup rocks (Sarkar *et al.* 1994). The rocks belonging to Dongargarh volcano-sedimentary successions are exposed to 40–50 km south of the present boninite dyke. Although both the dykes are intruded in different lithological units but their proximity may indicate that both the dykes are younger than the 2.14–2.18 Ga Bijli rhyolites (Sarkar *et al.* 1994; Divakara Rao *et al.* 2000) but older than the 1.86 Ga dyke swarm of the Bastar (Srivastava 2006). The southern Bastar boninites are also reported to be emplaced at 2118 ± 2 Ma (Srivastava *et al.* 2011). The analogous mineralogical and geochemical characteristics of the present dyke with the rest of the Bastar boninites may indicate similar mantle source regions for their genesis and thus
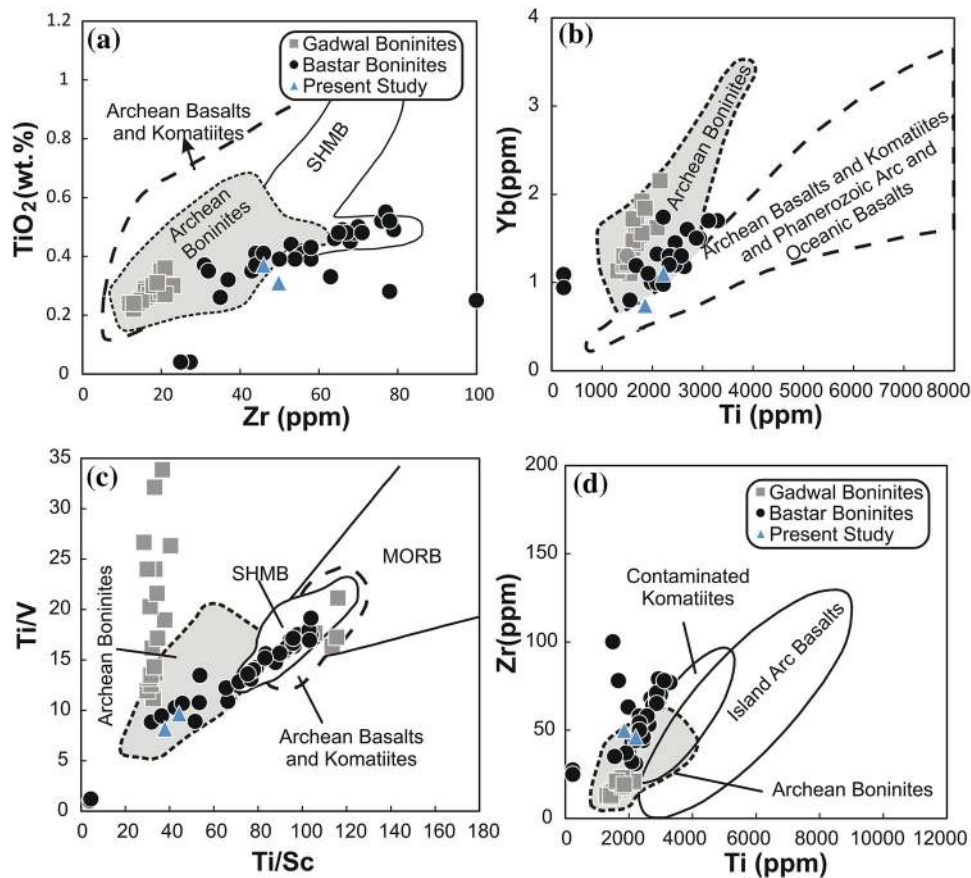

Figure 10. (**a**) Zr (ppm) *vs.* TiO₂ (wt.%), (**b**) Ti (ppm) *vs.* Yb (ppm), (**c**) Ti/Sc *vs.* Ti/V, and (**d**) Ti (ppm) *vs.* Zr (ppm) variation diagram for the present boninite dyke and their comparison with Archaean boninites, Gadwal boninites, Bastar boninites, SHMB, Archaean basalts and komatiites, Phanerozoic arc and oceanic basalts and MORB. Data from Poidevin (1994), Smithies (2002), Polat *et al.* (2002), Smithies *et al.* (2004), Manikyamba *et al.* (2005), Subba Rao *et al.* (2008a, b) and Chalapathi Rao and Srivastava (2009).

represent a widespread boninite intrusion event in the Bastar craton during the Palaeoproterozoic. The significant geochemical characteristics corresponding with subduction setting also suggest that like the Dongargarh boninite, the present dyke (along with north Bastar boninite) represents the preservation of ancient subduction-related signatures retained by the lithospheric mantle of this domain during the evolution of the Bastar craton and Dongargarh Supergroup.

8. Conclusions

The boninite dyke under study shows the presence of mafic minerals such as pyroxenes and amphiboles along with subordinate amounts of plagioclase. The pyroxenes are mostly diopside in composition (Wo_{48-50}), whereas amphiboles show the composition of actinolite and hornblende. It shows enrichment of LILEs along with depletion of HFSEs (Nb, Ti), and based on low TiO_2 (0.19–0.37 wt.%), higher CaO/Al_2O_3 (3.13–3.96) it is classified as high Ca boninite. These specific geochemical characteristics are consistent with the refractory mantle source formed by the extraction of basaltic magma during Archaean/Early Proterozoic times in the Bastar craton. The similarity of the present dyke with the earlier reported Bastar boninites and particularly with north Bastar boninite indicates the similar composition of the mantle source and a widespread Palaeoproterozoic boninitic event in the craton. This boninite magmatism indicates the presence of remnant subduction-related signatures in the lithospheric mantle formed during the evolution of the Bastar craton.

Acknowledgements

References

Arndt N T, Brügmann G E, Lenhert K, Chappel B W and Chauvel C 1987 Geochemistry, petrogenesis and tectonic environment of Circum-Superior Belt basalts, Canada; In: *Geochemistry and Mineralisation of Proterozoic Volcanic Suites* (eds) Pharaoh T C, Beckinsdale R D and Rickard D, Blackwell, London.

Asthana D, Dash M R, Pophare A M and Khare S K 1996 Interstratified low-Ti and high-Ti volcanics in the arc-related Khairagarh Group of central India; *Curr. Sci.* **71** 304–306.

Asthana D, Khare S K, Pophare A M and Dash M R 1997 Comments on – Geochemistry of the Dongargarh volcanic rocks, central India: Implications for the Precambrian mantle; *Precamb. Res.* **84** 105–107.

Asthana D, Kumar H, Balakrishnan S, Xia Q and Feng M 2016 An early cretaceous analogue of the ∼ 2.5 Ga Malanjkhand porphyry Cu deposit, central India; *Ore. Geol. Rev.* **72** 1197–1212.

Asthana D, Kumar S, Vind A K, Zehra F, Kumar H and Pophare A M 2017 Geochemical fingerprinting of ∼ 2.5 Ga forearc-arc-backarc related magmatic suites in the Bastar craton, central India; *J. Asian Earth Sci.,* https://doi.org/10.1016/j.jseaes.2017.10.006.

Beccaluva L and Serri G 1988 Boninitic and low-Ti subduction-related lavas from intraoceanic arc-backarc systems and low-Ti ophiolites: A reappraisal of their petrogenesis and original tectonic setting; *Tectonophys.* **146** 291–315.

Bedard J H 1999 Petrogenesis of Boninites from the Betts Cove Ophiolite, Newfoundland, Canada: Identification of subducted source components; *J. Petrol.* **40**(**12**) 1853–1889.

Cameron W E, McCulloch M T and Walker D A 1983 Boninite petrogenesis: Chemical and Nd–Sr isotopic constraints; *Earth Planet. Sci. Lett.* **65** 75–89.

Chalapathi Rao N V and Srivastava R K 2009 A new find of boninite dyke from the Paleoproterozoic Dongargarh Supergroup: Inference for a fossil subduction zone in the Archean of the Bastar craton, central India; *J. Mineral. Geochem.* **186**(**3**) 271–282.

Chaudhuri A K, Saha D, Deb G K, Deb S P, Mukherjee M K and Ghosh G 2002 The Purana basins of southern cratonic provinces of India a case for Mesoproterozoic fossil rifts; *Gondwana Res.* **5** 23–33.

Condie K C 1997 Sources of Proterozoic mafic dyke swarms: Constraints from Th/Ta and La/Yb ratios; *Precamb. Res.* **81** 3–14.

Crawford A J, Falloon T J and Green D H 1989 Classification, petrogenesis and tectonic setting of boninites; In: *Boninites and Related Rocks* (ed.) Crawford A J, Unwin Hyman, London, pp. 1–49.

Crookshank H 1963 Geology of southern Bastar and Jeypore from the Bailadila range to the Eastern Ghats; *Geol. Surv. India Memoir* **87** 150.

Das P, Das K, Chakraborty P P and Balakrishnan S 2011 1420 Ma diabasic intrusives from the Mesoproterozoic Singhora Group, Chhattisgarh Supergroup, India: Implications towards non-plume intrusive activity; *J. Earth Syst. Sci.* **120** 223–236.

Divakara Rao V, Narayana B L, Rama Rao P, Murthy N N, Subba Rao M V, Mallikharjuna Rao J and Reddy G L N 2000 Precambrian acid volcanism in central India – Geochemistry and origin; *Gondwana Res.* **3** 215–226.

Falloon T J and Danyushevsky L V 2000 Melting of refractory mantle at 1.5, 2 and 2.5 GPa under anhydrous and H_2O undersaturated conditions: Implications for the petrogenesis of high-Ca boninites and the influence of subduction components on mantle melting; *J. Petrol.* **41** 257–283.

Falloon T J, Danyushevsky L V, Crawford T J, Maas R, Woodhead J D, Eggins S M, Bloomer S H, Wright D J, Zlobin S K and Stacey A R 2007 Multiple mantle plume components involved in the petrogenesis of subduction-related lavas from the northern termination of the Tonga Arc and northern Lau Basin: Evidence from the geochemistry of arc and backarc submarine volcanics; *Geochem. Geophys. Geosyst.,* https://doi.org/10.1029/2007GC001619.

Falloon T J, Danyushevsky L V, Crawford A J, Meffre S, Woodhead J D and Bloomer S H 2008 Boninites and Adakites from the northern termination of the Tonga Trench: Implications for Adakite Petrogenesis; *J. Petrol.* **49** 697–715.

French J E, Heaman L M, Chacko T and Srivastava R K 2008 1891–1883 Ma Southern Bastar–Cuddapah mafic igneous events, India: A newly recognized large igneous province; *Precamb. Res.* **160** 308–322.

Ganguly S, Manikyamba C, Saha A, Lingadevaru M, Santosh M, Rambabu S, Khelen A C, Purushottam D and Linga D 2016 Geochemical characteristics of gold bearing boninites and banded iron formations from Shimoga greenstone belt, India: Implications for gold genesis and hydrothermal processes in diverse tectonic settings; *Ore. Geol. Rev.* **73** 82–89.

Gautam G C and Srivastava R K 2011 Petrology, geochemistry and petrogenesis of Early Precambrian mafic dyke swarm from Dondi–Bhanuprattapur–Keshkal, Central Bastar craton, India; In: *Dyke Swarms: Keys for Geodynamic Interpretation* (ed.) Srivastava R K, Springer-Verlag, Heidelberg, pp. 203–218.

Green D H and Falloon T J 1998 Pyrolite: A Ringwood concept and its current expression; In: *The Earth's Mantle: Composition, Structure and Evolution* (ed.) Jackson I, Cambridge University Press, Cambridge, pp. 311–378.

Green T H and Pearson N J 1986 Ti-rich accessory phase saturation in hydrous mafic-felsic compositions at high P–T; *Chem. Geol.* **54** 185–201.

Hall R P and Hughes D J 1990 Precambrian mafic dykes of southern Greenland; In: *Mafic Dykes and Emplacement Mechanisms* (eds) Parker A J, Rickwood D H, Tucker D H and Balkema A A, Rotterdam, pp. 481–495.

Hickey R L and Frey F A 1982 Geochemical characteristics of boninitic series volcanics: Implications for their source; *Geochim. Cosmochim. Acta* **46** 2099–2115.

Hussain F, Mondal M E A and Ahmad T 2004 Geodynamic evolution and crustal growth of the central Indian shield: Evidence from geochemistry of gneisses and granitoids; *J. Earth Syst. Sci.* **113** 699–714.

Hussain M F, Ahmad T and Mondal M E A 2008 Geochemistry of the Precambrian MAFIC DYKE SWARMS of the central and northeastern parts of Bastar Craton, central India: Constraints on their enrichment processes; In: *Indian Dykes: Geochemistry, Geophysics and Geochronology* (eds) Srivastava R K, Sivaji C and Chalapathi Rao N V, Narosa Publishing House Pvt. Ltd., New Delhi, pp. 397–412.

Krishnamurthy P, Chaki A, Pandey B K, Chimote J S and Singh S N 1988 Geochronology of the granite-rhyolite suite of the Dongargarh Supergroup, central India; In: *Fourth National Symposium on Mass Spectrometry*, Indian Institute of Science, Bangalore, EPS-2/1-3.

Krishnamurthy P, Sinha D K, Rai A K, Seth D K and Singh S N 1990 Magmatic rocks of the Dongargarh supergroup, central India – Their petrological evolution and implications on metallogeny; *Geol. Surv. India Spec. Publ.* **28** 303–319.

Kushiro I 2007 Origin of magmas in subduction zones: A review of experimental studies; *Proc. Jpn. Acad. Ser.* **83** 1–15.

Lafleche M R, Dupuy C and Bougault H 1992 Geochemistry and petrogenesis of Archean volcanic rocks of the southern Abitibi Belt, Quebec; *Precamb. Res.* **57** 207–241.

Leake B E, Woolley A R, Arps C E S, Birch W D, Gilbert M C, Grice J D, Hawthorne F C, Kato A, Kisch H J, Krivovichev V G, Linthout K, Laird J, Mandarino J A, Maresch W V, Nickel E H, Rock N M S, Schumacher J C, Smith D C, Stephenson N C N, Ungaretti L, Whittaker E J W and Youzhi G 1997 Nomenclature of amphiboles: Report of the subcommittee on amphiboles of the international mineralogical association, commission on new minerals and mineral names; *Am. Mineral.* **82** 1019–1037.

Le Bas M J 2000 IUGS reclassification of the high-Mg and picritic volcanic rocks; *J. Petrol.* **41** 1467–1470.

Manikyamba C, Naqvi S M, Subba Rao D V, Ram Mohan M, Khanna T C, Rao T G and Reddy G 2005 Boninites from the Neoarchaean Gadwal greenstone belt, Eastern Dharwar craton, India: Implications for Archaean subduction processes; *Earth Planet. Sci. Lett.* **23** 65–83.

Manikyamba C, Santosh M, Chandan Kumar B, Rambabu S, Tang L, Saha A, Khelen A, Ganguly S, Singh T D and Subba Rao D V 2016 Zircon U–Pb geochronology, Lu–Hf isotope systematic, and geochemistry of bimodal volcanic rocks and associated granitoids from Kotri belt, central India: Implications for Neoarchean–Paleoproterozoic crustal growth; *Gondwana Res.* **38** 313–333.

Meffre S, Falloon T J, Crawford T J, Hoernle K, Hauff F, Duncan R A, Bloomer S H and Wright D J 2012 Basalts erupted along the Tongan fore arc during subduction initiation: Evidence from geochronology of dredged rocks from the Tonga fore arc and trench; *Geochem. Geophys. Geosys.,* https://doi.org/10.1029/2012GC004335.

Melluso L and Sethna S F 2011 Mineral compositions of the Deccan igneous rocks of India: An overview; In: *Topics in Igneous Petrology* (eds) Ray J, Sen G and Ghosh B, Springer Science.

Merlet C 1994 An accurate computer correction program for quantitative electron probe microanalysis; *Microchim. Acta* **114/115** 363–376.

Mir A R, Alvi S H and Balaram V 2011 Geochemistry of the mafic dykes in parts of the Singhbhum Granitoid complex: Petrogenesis and tectonic setting; *Arab. J. Geosci.* **4** 933–943.

Mir A M, Alvi S H and Balaram V 2015 Boninitic geochemical characteristics of high-Mg mafic dykes from the Singhbhum granitoid complex, Eastern India; *Chin. J. Geochem.* **34**(**2**) 241–251.

Mondal M E A, Hussain M F and Ahmad T 2006 Continental growth of Bastar craton, central Indian shield during precambrian via multiphase subduction and lithospheric extension/rifting: Evidence from geochemistry of gneisses, granitoids and mafic dykes; *J. Geosci.* **49** 137–151.

Mondal M E A, Hussain M F and Ahmad T 2007 Geochemistry and petrogenesis of the Proterozoic mafic dyke swarms of Bastar craton of central Indian Shield; *J. Appl. Geochem.* **9** 17–27.

Naqvi S M and Rogers J J W 1987 *Precambrian geology of India*; Oxford University Press, Oxford, 233p.

Neogi S, Miura H and Hariya Y 1996 Geochemistry of the Dongargarh volcanic rocks, central India: Implications for the Precambrian mantle; *Precamb. Res.* **76** 77–91.

Nielsen S G, Joel A B and Krogstad E J 2002 Petrogenesis of an early Archaean (3.4 Ga) norite dyke, Isua, West Greenland: Evidence for early Archaean crustal recycling; *Precamb. Res.* **118** 133–148.

Pearce J A, van der Laan S R, Arculus R J, Murton B J, Ishii T, Peate D W and Parkinson I J 1992 Boninite and harzburgite from Leg 125 (Bonin-Mariana forearc): A case study of magma genesis during the initial stages of subduction; In: *Proceedings of the Ocean Drilling Program*, Scientific Results, **125** pp. 623–659.

Piercey S J, Murphy D C, Mortensen J K and Paradis S 2001 Boninite magmatism in a continental margin setting, Yukon–Tanana terrane, southeastern Yukon, Canada; *Geology* **29** 731–734.

Pisarevsky S A, Biswal T K, Wang X-C, De Waele B, Ernst R, Söderlund U, Tait J A, Ratre K, Singh Y K and Cleve M 2013 Palaeomagnetic, geochronological and geochemical study of Mesoproterozoic Lakhna Dykes in the Bastar Craton, India: Implications for the Mesoproterozoic supercontinent; *Lithos* **174** 125–143.

Poidevin J L 1994 Boninite-like rocks from the Paleoproterozoic greenstone belt of Bogoin, Central African Republic: Geochemistry and petrogenesis; *Precamb. Res.* **68** 97–113.

Polat A, Hofmann A W and Rosing M 2002 Boninite-like volcanic rocks in the 3.7–3.8 Ga Isua greenstone belt, West Greenland: Geochemical evidence for intra-oceanic subduction zone processes in the early Earth; *Chem. Geol.* **184** 231–254.

Ramachandra H M, Mishra V P and Deshmukh S S 1995 Mafic Dykes in Bastar Precambrian: Study of the Bhanupratappur–Keshkal Mafic Dyke Swarms; *Geol. Soc. India Mem.* **33** 183–208.

Ramakrishnan M 1990 Crustal development in southern Bastar, central India craton; *Geol. Surv. India Spec. Publ.* **28** 44–66.

Ramakrishnan M and Vaidyanadhan R 2008 Geology of India; *Geol. Soc. India* **1** 556.

Rao G V 1981 The correlation of the Dongargarh, Chilpi and Sausar Groups. *Geol. Surv. India Spec. Publ.* **3** 9–15.

Ratre K, De Waele B, Biswal T K and Sinha S 2010 SHRIMP geochronology for the 1450 Ma Lakhna dyke swarm: Its implication for the presence of Eoarchaean crust in the Bastar Craton and 1450–517 Ma depositional age for Purana basin (Khariar), Eastern Indian Peninsula; *J. Asian Earth Sci.* **39** 565–577.

Raza M, Jafri S H, Alvi S H and Khan M S 1993 Geodynamic evolution of the Indian shield during Proterozoic: Geochemical evidence from mafic volcanic rocks; *J. Geol. Soc. India* **41** 455–469.

Roy A, Ramachandra H M and Bandopadhyay B K 2000 Supracrustal belts and their significance in the crustal evolution of central India; *Geol. Surv. India Spec. Publ.* **55** 361–380.

Sarkar S N 1994 Chronostratigraphy and tectonics of the Dongargarh Supergroup Precambrian rocks in Bhandara-Durg region, central India; *Indian J. Earth Sci.* **21** 19–31.

Sarkar S N, Gopalan K and Trivedi J R 1981 New data on the geochronology of the Precambrians of Bhandara-Durg, central India; *Indian J. Earth Sci.* **8(2)** 131–151.

Sarkar G, Gupta S N and Bishui P K 1994 New Rb-Sr isotopic age and geochemistry of granite gneisses from southern Bastar craton: Implication for crustal evolution; *Indian Mineral.* **48** 7–12.

Sensarma S, Palme H and Mukhopadhyay D 2002 Crust–mantle interaction in the genesis of siliceous high magnesian basalts: Evidence from the early Proterozoic Dongargarh Supergroup, India; *Chem. Geol.* **187** 21–37.

Sinha D K, Jain S K and Naganath K P 2011 Tectonic significance and age of doleritic sill near Bandhalimal in the Singhora Protobasin of Chhattisgarh Basin, central India. In: *Dyke Swarms: Keys for Geodynamic Interpretation* (ed.) Srivastava R K, Springer-Verlag, Heidelberg, pp. 167–187.

Smellie J L, Stone P and Evans J 1995 Petrogenesis of boninites in Ordovician Ballantrae complex Ophiolite, south western Scotland; *J. Volcano. Geotherm. Res.* **69** 323–342.

Smithies R H 2002 Archaean boninite-like rocks in an intracratonic setting; *Earth Planet. Sci. Lett.* **197** 19–34.

Smithies R H, Champion D C and Sun S S 2004 The case of Archaean boninites; *Contrib. Mineral. Petrol.* **147** 705–721.

Srivastava R K 2006 Geochemistry and petrogenesis of Neoarchaean high-Mg low-Ti mafic igneous rocks in an intracratonic setting, central India craton: Evidence for Boninite magmatism; *Geochem. J.* **40** 15–31.

Srivastava R K 2008 Global intracratonic boninite-norite magmatism during the Neoarchean-Paleoproterozoic: Evidence from the central Indian Bastar craton; *Int. Geol. Rev.* **50** 61–74.

Srivastava R K and Gautam G C 2008 Precambrian mafic dyke swarms from the southern Bastar central India craton: Present and future perspectives. In: *Indian dykes: Geochemistry, geophysics and geochronology* (eds) Srivastava R K, Sivaji C and Chalapathi Rao N V, Narosa Publishing House Pvt. Ltd., New Delhi, pp. 367–376.

Srivastava R K and Gautam G C 2009 Precambrian mafic magmatism in the Bastar craton, central India; *J. Geol. Soc. India* **73** 52–72.

Srivastava R K and Gautam G C 2012 Early Precambrian mafic dyke swarms from the Central Archaean Bastar craton, India: Geochemistry, petrogenesis and tectonic implications; *Geol. J.* **47** 144–160.

Srivastava R K and Gautam G C 2015 Geochemistry and petrogenesis of Paleo-Mesoproterozoic mafic dyke swarms from northern baster Craton, central India: Geodynamic implication in reference to Columbia supercontinent; *Gondwana Res.* **28** 1061–1078.

Srivastava R K and Singh R K 2003 Geochemistry of high-Mg mafic dykes from the Bastar craton: Evidence of Late Archaean boninite-like rocks in an intracratonic setting; *Curr. Sci.* **85** 808–812.

Srivastava R K and Singh R K 2004 Trace element geochemistry and genesis of the Precambrian sub-alkaline mafic dykes from central India craton: Evidence for mantle metasomatism; *J. Asian Earth Sci.* **23** 373–389.

Srivastava R K, Singh R K and Verma S P 2004 Late Archaean mafic volcanic rocks from the southern Bastar greenstone belt, central India: Petrological and tectonic significance; *Precamb. Res.* **131** 305–322.

Srivastava R K, Heaman L M, French J E and Ferreira Filho C F 2011 Evidence for a Paleoproterozoic event of metamorphism in the Bastar craton, central India: P-T-t constraints from mineral chemistry and U-Pb geochronology of mafic dykes; *Episodes* **34**(**1**) 13–24.

Stern R J and Bloomer S H 1992 Subduction zone infancy: Examples from the Eocene Izu–Bonin–Mariana and Jurassic California arcs; *Geol. Soc. Am. Bull.* **104**(**12**) 1621–1636.

Subba Rao D V, Balaram V, Charan S N, Sridhar D N and Naqvi S M 2004 Proterozoic mafic dykes in and around Chattisgarh basin, central India: Inferences of compositional variation in mantle sources; *DST-DCS News Lett.* **14** 1–5.

Subba Rao D V, Sridhar D N, Balaram V, Nagaraju K, Rao T G, Keshavakrishna A and Singh U P 2008a Proterozoic mafic–ultramafic dyke swarms in the vicinity of Chattisgarh–Khariar–Singhora basins in Northern Bastar craton, central India; In: *Indian Dykes: Geochemistry, Geophysics and Geochronology* (eds) Srivastava R K, Sivaji C and Chalapathi Rao N V, Narosa Publishing House, New Delhi, pp. 377–396.

Subba Rao D V, Balaram V, Nagaraju K and Sridhar D N 2008b Palaeoproterozoic boninite like rocks in an intracratonic setting from Northern Bastar craton, central India; *J. Geol. Soc. India* **72** 373–380.

Sun S S and McDonough W 1989 Chemical and isotopic systematics of oceanic basalts: Implications for mantle composition and processes; In: *Magmatism in Ocean Basins* (eds) Saunders A D and Norry M J, *Geol. Soc. London Spec. Publ.* **42** 313–345.

Sun S S and Nesbitt R W 1978 Petrogenesis of Archaean ultrabasic and basic volcanism: Evidence from rare earth elements; *Contrib. Mineral. Petrol.* **65** 301–325.

Sun S S, Nesbitt R W and McCulloch M T 1989 Geochemistry and petrogenesis of Archaean and early Proterozoic siliceous high magnesian basalts. In: *Boninites and Related Rocks* (ed.) Crawford A J, Unwin Hyman, London, pp. 148–173.

Tatsumi Y and Eggins S 1995 *Subduction Zone Magmatism*; Blackwell Science, Oxford, 211p.

Turner S, Hawksworth G, Rogers N, Barlett J, Worthington T, Hergt G, Pearce J and Smith I 1997 ^{238}U–^{230}Th disequilibria, magma petrogenesis, and flux rates beneath the depleted Tonga–Karmadec island-arc; *Geochim. Cosmochim. Acta* **61** 4884–4885.

Wanjari N, Asthana D and Divakara Rao V 2005 Remnants of early continental crust in the Amgaon gneisses, central India: Geochemical evidence; *Gondwana Res.* **8** 589–595.

Wilson M 1989 *Igneous Petrogenesis: A Global Tectonic Approach*; Unwin Hyman, London, 466p.

Yedekar D P, Jain S C, Nair K K K and Dutta K K 1990 The central Indian collision suture; *Geol. Surv. India Spec. Publ.* **28** 1–43.